

ABSTRACT

PERFORMANCE ANALYSIS OF SPACE-TIME TRELLIS CODED
MIMO-OFDM SYSTEMS

By

Samet Yildiz

May 2015

Space-time codes are a standout amongst the most prominent procedure utilized as a part of the multiple-input multiple-output (MIMO) systems in the advanced communication systems. While ordinary transmission between one transmit and one receive antenna is utilized, one can see neither diversity gain nor coding gain, which eventually implies that a critical change in the transmission cannot be observed. Space-time codes can be effectively connected through multiple transmit antennas and optional number of receive antennas. There are several approaches to provide diversity gain. The researches which are developed to achieve diversity gain by late 1990's are called as space-time block codes (STBC). Despite the fact that the STBC is anything but easy to execute, they do not provide any coding gain. Subsequently, so as to accomplish the coding gain other than the diversity gain, the space-time trellis codes (STTC) are connected all through this theory. STTC, which gives coding gain in regards to the number of the states, is then joined with the orthogonal frequency division multiplexing (OFDM) systems, which is a prominent transmission method to send orthogonal signals with no interference between the subcarriers. It is ultimately called as STTC-OFDM systems.

PERFORMANCE ANALYSIS OF SPACE-TIME TRELLIS CODED
MIMO-OFDM SYSTEMS

A THESIS

Presented to the Department of Electrical Engineering
California State University, Long Beach

In Partial Fulfillment
of the Requirements for the Degree
Master of Science in Electrical Engineering

Committee Members:

Yeh, Hen-Geul, Ph.D. (Chair)
Mangir, Tulin , Ph.D.
Mozumdar, Mohammad , Ph.D.

College Designee:

Antonella Sciortino, Ph.D.

By Samet Yildiz

B.S., 2012, Yeditepe University

May 2015

UMI Number: 1587932

All rights reserved

INFORMATION TO ALL USERS

The quality of this reproduction is dependent upon the quality of the copy submitted.

In the unlikely event that the author did not send a complete manuscript and there are missing pages, these will be noted. Also, if material had to be removed, a note will indicate the deletion.



UMI 1587932

Published by ProQuest LLC (2015). Copyright in the Dissertation held by the Au

Microform Edition © ProQuest LLC.

All rights reserved. This work is protected against
unauthorized copying under Title 17, United States Code



ProQuest LLC.
789 East Eisenhower
Parkway
P.O. Box 1346

ACKNOWLEDGEMENTS

I might want to express my deepest appreciation and gratefulness to my family for supporting me in any case. I additionally acknowledge to my friends from Turkey and Long Beach, who have continually been supporting me profoundly for my education. I am truly appreciative of my friends in our MIMO group in CSULB who talked about with and provided for me some advice about my thesis. Last but not least, if it were not for Dr. Hen-Geul Yeh and his constant supervision, direction, and help, this thesis would have been so much more challenging to me.

TABLE OF CONTENTS

	Page
ACKNOWLEDGEMENTS	iii
LIST OF FIGURES	vi
CHAPTER	
1. INTRODUCTION	1
2. WIRELESS CHANNEL MODELS	4
AWGN Channel Model.....	5
Rayleigh Fading Channel Model.....	6
3. SPACE-TIME TRELLIS CODES	10
Coding Gain Versus Diversity Gain	10
General Space-Time Trellis Code System Model.....	12
STTC Encoder.....	16
STTC Performance Analysis and Design Criteria.....	20
4. OFDM SYSTEMS	25
Overview of the OFDM Systems	25
Mathematical Model of a Traditional OFDM System	26
MIMO-OFDM Channel Models	30
5. THE SIMULATION OF STTC-OFDM OVER FREQUENCY SELEC- TIVE FADING CHANNEL MODEL	31
STTC-OFDM Simulation Parameters	31
STTC-OFDM Transmitter.....	31
STTC-OFDM Channel Model.....	32
STTC-OFDM Receiver.....	34
STTC-OFDM Versus ST-OFDM.....	35
6. THE FUTURE IMPLEMENTATIONS FOR STTC-OFDM SYSTEMS	40
STTC-PC-OFDM Systems	41
STTC-CC-OFDM Systems	42
STTC-CPC-OFDM Systems.....	42
Future Works	43

	Page
7. CONCLUSION AND RECOMMENDATIONS	45
REFERENCES	47

LIST OF FIGURES

FIGURE	Page
1. AWGN Channel Model.	5
2. Rayleigh Fading Channel Tap Model.	9
3. Delay Diversity Transmitter Block Diagram.	12
4. A QPSK Constellation Representation.	13
5. Simple 4 State QPSK Trellis Diagram.....	13
6. QPSK Trellis Diagrams for 4, 8 and 16 States.	14
7. Block Diagram of an STTC Transceiver Model.....	15
8. STTC Encoder for M -PSK Systems.....	17
9. STTC for QPSK with 2 Transmit and 1 Receive Antenna.....	18
10. STTC for QPSK with 2 Transmit and 2 Receive Antenna.....	19
11. Traditional OFDM Transmitter Block Diagram.	27
12. Traditional OFDM Receiver Block Diagram.	28
13. Multiple Antenna Transceiver Block Diagram.	29
14. 2-Tx & 1-Rx STTC-OFDM System.	32
15. ST-OFDM vs STTC-OFDM with $f_D = 0Hz$	37
16. ST-OFDM vs STTC-OFDM with $f_D = 200Hz$ ($5\mu s$ delay spread). ...	38
17. ST-OFDM vs STTC-OFDM with $f_D = 200Hz$ ($40\mu s$ delay spread)...	39
18. 2-Tx & 1-Rx Regular ST-OFDM System.	40
19. 2-Tx & 1-Rx STTC-PC-OFDM System.....	41

FIGURE	Page
20. 2-Tx & 1-Rx STTC-CC-OFDM System.....	42
21. 2-Tx & 1-Rx STTC-CPC-OFDM System.....	43

CHAPTER 1

INTRODUCTION

The wireless business has begun to climb from its root a century ago. One can say that the wireless systems are the key factors of the technology. People started to search for different methods to have an internet access on account of new technologies. Thus, the twentieth century provided novel silicon innovations, which gives more speed and more reliability in the wireless system design. A ton of scientific hypotheses were built to give better utilization of it. The acknowledgement of the hypotheses into the wireless area began to require more bandwidth and better spectral utilize. At the end of the day, the conventional single-input single-output (SISO) systems were modified with quite a few smart modifications.

Most importantly, keeping in mind the end goal to alter the current SISO system better, there is a need for understanding the real world effects, which are called as channel effects. The Rayleigh statistical approach is a prominent strategy to find the channel effects. This thesis solely uses Rayleigh channel models. Considering the possible channel impacts, for example, fading, scattering, and so forth, one can consider renovating the existing transmitter and receiver structure. Single-input multiple-output (SIMO), multiple-input single-output (MISO) and multiple-input multiple-output (MIMO) transceiver structure can be adopted with respect to this. The channel knowledge information only at the receiver in multiple antenna arrangement has pulled in a ton of research attentions [1].

The receiver diversity was a favored system for the SIMO setup with the utilization of maximal ratio combining (MRC) method before the transmit diversity was embraced. Since the receive diversity is an expensive choice, the transmit diversity was pulled in a few looks into utilizing transmit diversity with the coding methods in 1995 [2], followed by Tarokh, Seshadri and Calderbank in 1998 [3]. They brought the space-time coding concept into the corresponding literature which they called as space-time trellis codes (STTC). This paper was followed by Alamouti's paper [4], which is known as space-time block codes (STBC).

While antenna setup was modified to maintain the diversity, frequency division multiplexing strategies in digital communication called orthogonal-frequency division multiplexing (OFDM) is also considered to improve the diversity further [5]. OFDM is a subgroup of frequency division multiplexing where a single channel is used through various sub-carriers on adjacent frequencies. This basically lessens the inter-symbol interference (ISI) on account of multiple carrier transmission. OFDM systems were executed on SISO systems which gave an outstanding performance in the transmission. After multiple antenna concept's entering in the digital communication systems, OFDM was beginning to be connected with the space-time coding systems [6]. After this consideration, they were started to be called as MIMO-OFDM in general.

There are great numbers of studies produced for MIMO-OFDM systems on the behalf of space-time codes [7]. Furthermore, another concept for MIMO-OFDM communication is derived which combats the inter carrier interference (ICI) due to the frequency offset with a smart modification at the transmitter and the receiver. Yeh and Yao [8] calls this concept as parallel cancellation. Parallel cancellation can be also modified with a slightly different way with the name of conjugate

cancellation. Lastly, one can combine both parallel and conjugate cancellation at the top of the STTC. For that reason, this thesis offers a novel of STTC coded MIMO-OFDM structure with the use of these ICI cancellation types.

This thesis is organized as follows. Initially, MIMO wireless channels are portrayed. Next, STTC is clarified with the different criteria. Then, the MIMO-OFDM systems are taken into the extent of the space-time codes. Subsequently, all matters examined here are coordinated which drives the reader to observe ST-OFDM (Space-time OFDM), STTC-OFDM (Space-time trellis coded OFDM), STTC-PC-OFDM (Space-time trellis coded parallel cancellation OFDM), STTC-CC-OFDM (Space-time trellis coded conjugate cancellation OFDM) and STTC-CPC-OFDM (Space-time trellis coded conjugate parallel cancellation OFDM) results with the Matlab simulations under the various conditions. Finally, last remarks and advice are offered about the future topics.

CHAPTER 2

WIRELESS CHANNEL MODELS

Wireless channels are the physical media between the transmitter and the receiver. The transmission between these two stations can be given through electromagnetic wave radiation, which are presented to several troubles such as reflection, scattering and diffraction. These matters make the electromagnetic waves encountering different path loss and phases. The received signals are super-positioned at the receiver, which causes an additive white Gaussian noise (AWGN) channel model. Despite the fact that the nature has random characteristics in every case, including the effects in the transmission, there are a few statistical ways to break down the channel models. In other words, signal propagation is characterized regarding to variations in the channel magnitude over time and frequency. These variations are basically defined as attenuation or (large scale fading) and just fading or (small scale fading).

Attenuation is essentially a continuous loss in the signal quality due to numerous reasons. So, it is more of a concern of deterministic approaches. To handle the channel model statistically, the motivation here will be just on a small scale fading. The small scale fading channels can be ordered in light of their time delay between their multipaths over the tap channel models. These multipaths occur because of the time delay coefficient in the channel model. They can be likewise grouped further based on their Doppler spread. The more comprehensive literature can be figured out in Sklar [9]. The utilized techniques as parts of the overall system are AWGN and Rayleigh channel models which are clarified later.

AWGN Channel Model

AWGN is a channel model which is the statistically wide frequency ranged random noise in a corresponding framework where a signal is influenced. It can be considered the AWGN noise only at the receiver. So, one can derive a numerical expression for the signal at the receiver input. The signal is corrupted by the channel because of the addition of white Gaussian noise as outlined in Figure 1.

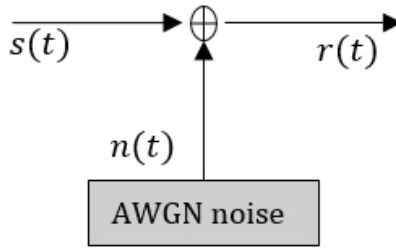


FIGURE 1. AWGN Channel Model.

When the transmitted signal is characterized as $s(t)$, the white Gaussian noise as $n(t)$, and the received signal as $r(t)$ which can be seen by equation 2.1.

$$r(t) = s(t) + n(t) \quad (2.1)$$

The probability density function (*pdf*) and power spectral density (*psd*) of $n(t)$ are derived as follows:

$$\phi_{nn}(f) = \frac{1}{2} N_o [W/Hz] \quad (2.2)$$

where N_o is called as one sided noise power density because of its steady nature. The Gaussian noise can be effortlessly produced by means of implicit *randn* function in the Matlab. Be that as it may, to give the impact of the AWGN

channel more reasonable, the noise variation must be considered when computing it. In this way, the variable $npow$ is characterized for the noise power. For including the impact of the noise power, the notation of $npow$ can be changed from power to voltage. That is the reason, one can infer the variable $attn$ from $npow$.

$$attn = \frac{1}{2}\sqrt{npow} \quad (2.3)$$

After calculating $attn$ with respect to equation 2.3, the noise-contaminated received signal $r(t)$ can be rearranged as can be seen from equation 2.4,

$$r(t) = s(t) + attn * n(t) \quad (2.4)$$

This notation is just clarified in SISO case. In the simulations, 3dB attenuation is additionally considered for 2 transmit antennas in order to make a fair comparison with SISO case. The noise variation varies in different instances of the antenna transmission. It will be clarified in the later parts [10].

Rayleigh Fading Channel Model

In order to comprehend the Rayleigh flat fading and Rayleigh frequency selective fading channels, there is a requirement for looking into the statistical portrayal of the fading channels. In the later chapters, STTC and OFDM are analyzed with different methodologies as indicated by the channel models.

Most importantly, fading channels can be acknowledged as linear time-varying systems where the time variations are random. Considering that the most wireless systems embrace bandpass transmission with the center carrier frequency of f_c . Therefore, one can understand this model utilizing a time-varying impulse response system. As such, the channel response at time t is seen by being

connected with an impulse at time $t - \tau$ in the time domain, or using a time - varying frequency response in the frequency domain.

Consider the bandpass transmitted signal by $x(t)$, and its low-pass part by $x_l(t)$. They can be spoken to as takes after:

$$x(t) = \text{Re}\{x_l(t)e^{j2\pi fct}\}. \quad (2.5)$$

In the event that the channel impulse response is shown by $h(\tau; t)$, the received signal is basically represented by equation 2.6 as a convolution between the transmitted signal and the channel impulse response with disregarding the noise.

$$y_l(t) = \int_{-\infty}^{+\infty} h(\tau; t)x_l(t - \tau) d\tau. \quad (2.6)$$

One can likewise consider the channel as a time-varying filter. Concerning this, the transfer function of the system is considered as the desired fading segment [11]. Besides, the Fourier transform of the channel impulse response can be inferred as for τ in equation 2.7.

$$H(f; t) = \int_{-\infty}^{+\infty} h(\tau; t)e^{-j2\pi f\tau} d\tau. \quad (2.7)$$

It can be reasoned that both $h(\tau; t)$ and $H(f; t)$ are a complex Gaussian random methodology. For time-domain operations, $h(\tau; t)$ is considered. In like manner, $H(f; t)$ is utilized for frequency-domain operations. They will further be clarified all through in the MIMO-OFDM system models in Chapter 4. In the wake of analyzing the continuous-time domain representation of the system, one

can surely modify it for the discrete-time model. Detailed discussion about channel models can be found from Sklar [9].

If the channel is described by the discrete-time representation, which this thesis embraces, one can make a simple move from time representation to tap channel representation. The channel impulse response in the discrete-time domain can be explained for this situation as takes after:

$$h(t, \tau) = \sum_{l=0}^{L-1} q(t, l) \delta(t - n_l T_s). \quad (2.8)$$

Tapped-delay line channel model is uncovered by equation 2.8 [12]. Here, $q(t, l)$ is the complex coefficient of the $l - th$ tap with the integer delay n_l . T_s is the sampling time of the proposed systems. In the wake of giving this general tapped delay line channel model, one can order this model with respect to the quantity of the taps to see the impacts of the channel.

Flat Fading (Single-Tap) Rayleigh Channel Model

It is evident that a single-tap channel model has a tap which has zero delay, or is called as line-of-sight (LOS) coefficient. As it were, it has one and only coefficient, which is ($l = 0$) coefficient, which gives no delay path. Also, $q(t, l)$ is displayed by the complex Gaussian process with variance $\sigma_l^2 = 1$ same as AWGN noise. That is the reason, why it is called flat fading. To demonstrate this, $L = 1$ can be given in equation 2.8 and be accomplished the outcome as an independent complex Gaussian coefficient.

Frequency Selective (Multi-Tap) Rayleigh Channel Model

Frequency selective channel model, then again, has more than one tap, which incorporates a delay part on every tap aside from the first (LOS) tap. Delay containing taps are called as non-line of sight taps (NLOS). The channel gets to be

subject to the delay and the sampling time of the overall system. Figure 2 highlights what the tap channel model looks like in work by Harada and Prasad [10]. By acquiring these channel models, one can design the space-time

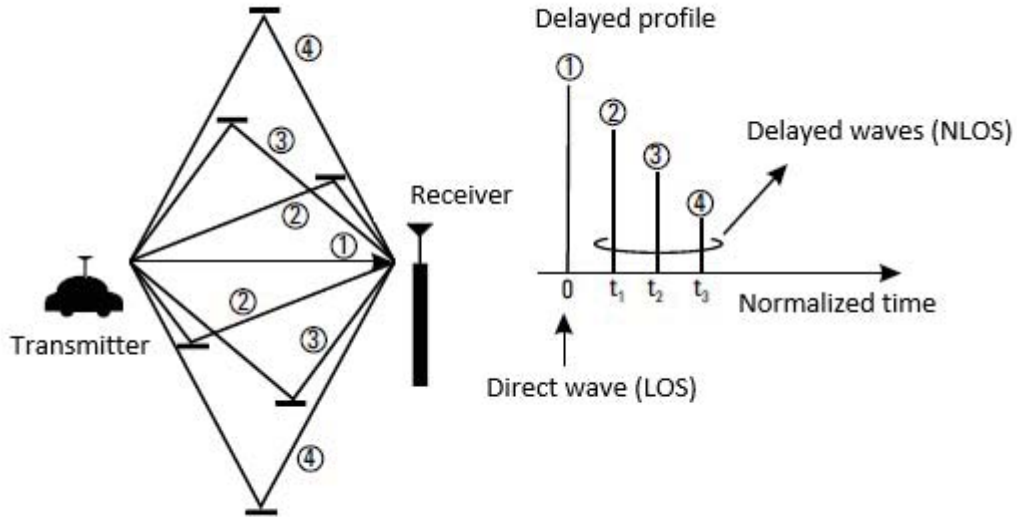


FIGURE 2. Rayleigh Fading Channel Tap Model.

trellis transceiver as per attain to desired performance. The single-tap channel model is the most straightforward type of the channel models. It is observed as a constant during one frame. Notwithstanding, it is a perfect case to consider. Hence, it is the key to execute space-time trellis codes over the frequency selective fading channels. The first performance criterion was designed as for a single-tap channel model shown by Tarokh et al. [3]. A short time later, there is truly a couple of examination analyzed the multi-tap channel effects inside the space-time trellis codes. The performance of the overall system through the tap-channel model will be clarified further.

CHAPTER 3

SPACE-TIME TRELLIS CODES

At the point when the space-time is considered, the diversity is recalled at first. Space-time block codes (STBC) give a diversity increase related to the number of transmit antennas. It gives way preferred performance over utilizing SISO case. MRC was an acknowledged technique before space-time codes were discharged. Since the MRC technique obliges various receive antennas to advance bit-error rate (BER) performance, the aggregate cost of the overall system grows exponentially. It implied, as it were, more antenna contained clients can benefit the transmit antenna more, which is seen as more cash, more performance. On the other hand, after space-time codes (STC) were discharged, the same performance was accomplished by the multiple transmit antennas. In STCs, there are neither redundant bits nor redundant waveforms. Alamouti clarified this well [4].

In spite of the fact that the STBC is generally easy to implement, it does not give any coding gain. Henceforth, space-time trellis codes (STTC) are applied to give both coding gain and diversity gain. Before beginning to clarify STTC, it is noteworthy to demonstrate the contrasts between coding gain and diversity gain in place for comprehension why the STTC can be favored over the STBC.

Coding Gain Versus Diversity Gain

The diversity gain can be observed where the multiple transmit or receive antennas are utilized. With the STBC, the transmit diversity is accomplished. It increases the slope of the BER curve. In the event that the channel model is changed over into the AWGN, it is difficult to see the diversity gain. Besides,

diversity diminishes the fading fluctuation, which is a compelling gain. Diversity gain can be arrived at not just by the blend of the independent replicas of a signal, additionally by the STCs. A definition of diversity gain is exhibited in the literature by Duman and Ghrayeb [11],

$$DiversityGain = - \lim_{SNR \rightarrow \infty} \frac{\log(PEP)}{\log(SNR)}. \quad (3.1)$$

This equality can be gotten from the relation between the transmitted and the received codes. According to equation 3.2, the pairwise error probability (PEP) can be derived, which is going to be explained later in this chapter. Also, the SNR is the signal to noise ratio in decibel (dB) scale. The SNR is essentially demonstrated as,

$$SNR_{dB} = 10 \log_{10} \frac{P_{signal}}{P_{noise}}. \quad (3.2)$$

Coding gain is an advantage taken from a coded system contrasted with the uncoded system having the same diversity. It speaks to left-shifted BER curve. Its impacts can be accomplished any sorts of channels. Coding gain gives less SNR utilization. Besides, it can be accomplished in various ways. Using redundant code sequence is one approach to obtain delay diversity. Memory using and waveform selection are used to provide different coding gains. Notwithstanding the way that the Alamouti STBC is anything but easy to implement, it does not give any coding gain. Like diversity gain, coding gain can be gotten from an upper bound PEP.

A vital conclusion can be made for the diversity and the coding gain in the light of the above definitions. Diversity is a technique to combat the ups and downs of the fading channels. However, it cannot give any commitment to the

AWGN-only channel. Then again, coding is a procedure which lessens the noise impact of the transmission. It can work in either fading or non-fading channels.

General Space-Time Trellis Code System Model

Consider a MIMO system with N transmit antennas and M receive antennas over the quasi-static flat fading channel. At every time instant t , m binary information are fed into the STTC encoder. STTC encoder takes these m -bits of symbols at every time instant one-by-one and transmits through N transmit antenna subsequently. The least difficult instance of STTC was made through delay diversity before Tarokh summed up the STTC idea [13]. For $N = 2$ transmit antennas, one of them has the delayed version of the same symbol stream as seen in Figure 3.

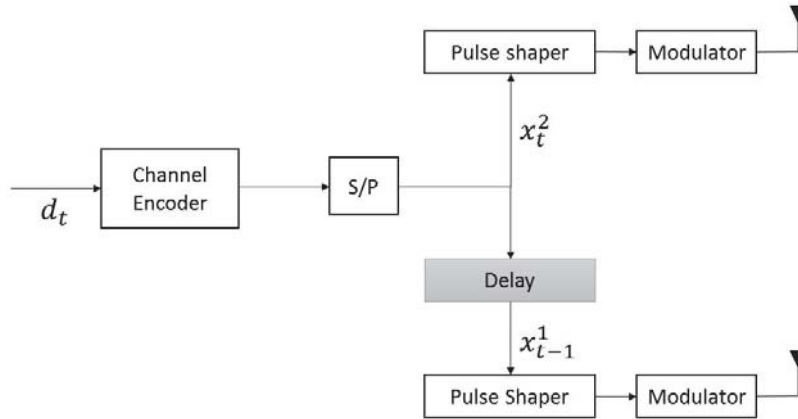


FIGURE 3. Delay Diversity Transmitter Block Diagram.

The basic 2 transmit antenna delay diversity (DD) scheme is later called as a 4-state space-time trellis codes. Using just DD scheme could not give a good performance and a coding gain. Therefore, the STTC principles were initially dispatched by Tarokh et al. [3] using trellis representation both in the encoder and the decoder. Consider a straightforward quadrature phase shift keying (QPSK)

which has the representation for coding the bit pairs like (00 = 1, 01 = +j, 10 = -1, 11 = -j). One can cover this representation to be utilized as a part of the trellis as seen in Figure 4.

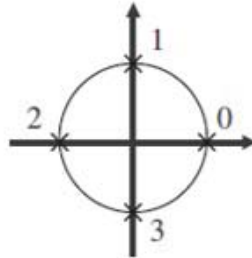


FIGURE 4. A QPSK Constellation Representation.

Starting from renaming the constellation, one can make the move from this constellation to the trellis with the given idea in Figure 5 which represents a 4-state QPSK trellis.

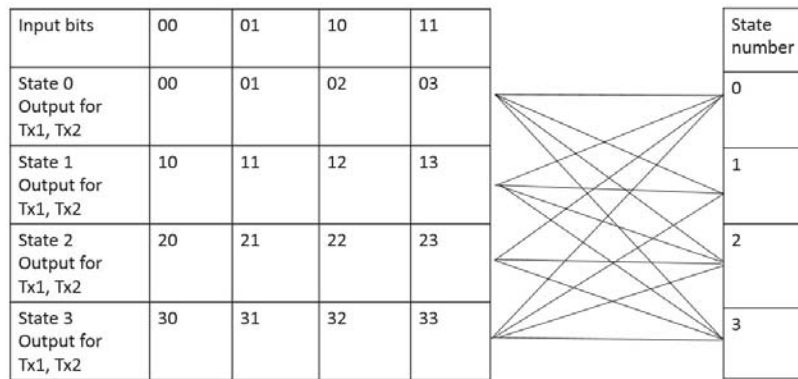


FIGURE 5. Simple 4 State QPSK Trellis Diagram.

In general, the trellis is represented with a simple trellis drawing. Regarding to this, one can say that the greater the number of the states, the better the system performance. The Figure 6 represents 4, 8 and 16 states of trellis representations.

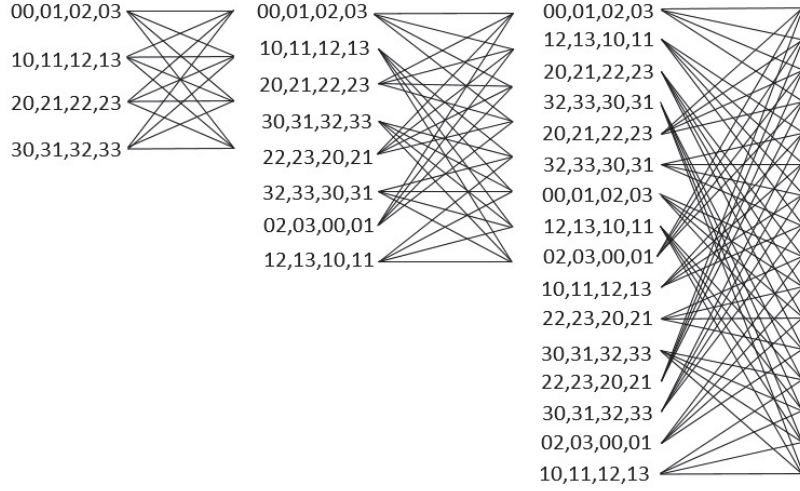


FIGURE 6. QPSK Trellis Diagrams for 4, 8 and 16 States.

With a basic way, the first and last bits of the serial input data symbols ($d_t = d_t^1, d_t^2, \dots, d_t^m$) at time t are set as zero to make sure that the encoder is cleared out and started from zero state again. After this, ($d_t = d_t^1, d_t^2, \dots, d_t^m$) symbol stream at every time instant t is encoded by an encoder with the trellis structure demonstrated in Figure 5. Next, the encoder gives N different branches transmitting at every t instant simultaneously in the meantime. The encoded code sequence $(x_t = x_1^t, x_2^t, \dots, x_N^t)^T$ is transmitted from every transmit antenna separately. The channel is assumed as a quasi-static fading channel, which is an $M \times N$ matrix. The channel matrix, H at time t is given by,

$$H_t = \begin{pmatrix} h_{1,1}^t & h_{1,2}^t & \dots & h_{1,N}^t \\ h_{2,1}^t & h_{2,2}^t & \dots & h_{2,N}^t \\ \vdots & \vdots & \ddots & \vdots \\ h_{M,1}^t & h_{M,2}^t & \dots & h_{M,N}^t \end{pmatrix} \quad (3.3)$$

The received code sequence can be named after passing through the channel at time t as $(y_t = y_1^t, y_2^t, \dots, y_M^t)^T$. The AWGN noise is likewise considered, which has the same size with received signal as $(n_t = n_1^t, n_2^t, \dots, n_M^t)^T$. One can put all the variables together at time t , which gives the received signal at antenna $j = 1, 2, \dots, M$ with the following equation:

$$y_t^j = \sum_{i=1}^N h_{j,i}^t x_t^i + n_t^j. \quad (3.4)$$

The equation 3.4 can be envisioned as seen in Figure 7. It speaks to the STTC transceiver model. It can be additionally disentangled as a matrix notation in equation 3.5.

$$y_t = H_t x_t + n_t. \quad (3.5)$$

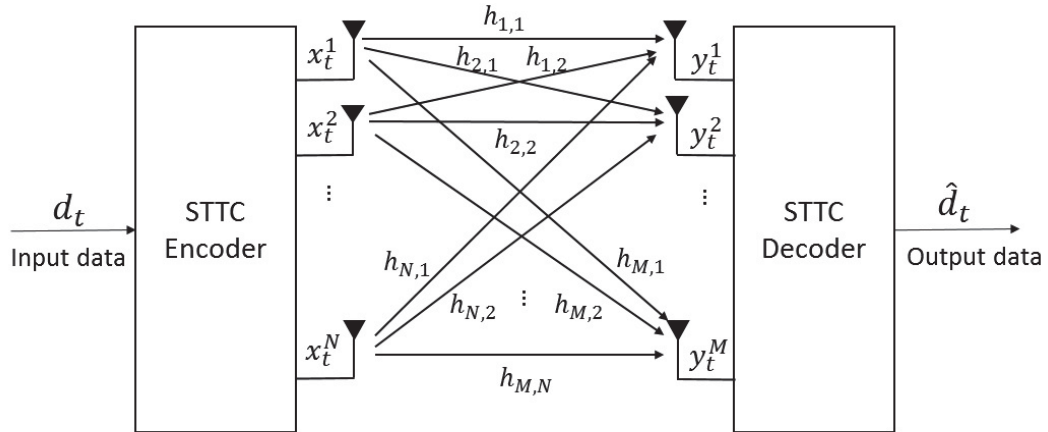


FIGURE 7. Block Diagram of an STTC Transceiver Model.

To give a superior understanding of equation 3.5, one can place them into the matrices, which are further written as in equation 3.6:

$$\begin{pmatrix} y_t^1 \\ y_t^2 \\ \vdots \\ y_t^M \end{pmatrix}_{M \times 1} = \begin{pmatrix} h_{1,1}^t & h_{1,2}^t & \dots & h_{1,N}^t \\ h_{2,1}^t & h_{2,2}^t & \dots & h_{2,N}^t \\ \vdots & \vdots & \ddots & \vdots \\ h_{M,1}^t & h_{M,2}^t & \dots & h_{M,N}^t \end{pmatrix}_{M \times N} \times \begin{pmatrix} x_t^1 \\ x_t^2 \\ \vdots \\ x_t^N \end{pmatrix}_{N \times 1} + \begin{pmatrix} n_t^1 \\ n_t^2 \\ \vdots \\ n_t^M \end{pmatrix}_{M \times 1} \quad (3.6)$$

The received signal can be decoded using maximum-likelihood decoding algorithm. Viterbi algorithm effortlessly solves the maximum-likelihood decoding with a memory efficient way [9]. To estimate the transmitted code sequence, the receiver is assumed to have a perfect channel state information (CSI). In any case, none of the transmitters have the channel state information. The CSI parameters are used to process the branch metric in the decoder with the same trellis structure defined in the STTC encoder at the transmitter part. The branch metric is figured taking into account the squared Euclidean distance between the received signal y_t and all possible trellis paths which are now reproduced by H . The estimated code sequence \hat{d}_t is indicated as,

$$\hat{d}_t = \underset{d_t}{\operatorname{arg\,min}} \left(\sum_{j=1}^M |y_t^j - \sum_{i=1}^N h_{j,i}^t q_t^i|^2 \right). \quad (3.7)$$

where the q_t^i is the possible trellis paths which can be observed from the Figure 6. The Viterbi algorithm chooses the best possible minimum distance from the defined trellis and estimates the input symbols regarding to equation 3.7 [14].

STTC Encoder

Consider an STTC encoder for M -PSK modulated symbols which give $m = \log_2 M$ bit pairs for every symbol with N transmit antennas. The encoder maps the symbol stream $(d_t = d_t^1, d_t^2, \dots, d_t^m)$ as $(x_t = x_1^t, x_2^t, \dots, x_N^t)^T$ which are transmitted all the while in the meantime from N transmit antennas.

Generator Matrix Representation

The STTC encoder in Figure 7 receives $(d_t = d_t^1, d_t^2, \dots, d_t^m)$ bit pairs of the symbols at every time instant t . They are fed into m feed forward shift registers and multiplied by a set of encoder coefficients. This model can likewise be showed with a generator matrix representation. Figure 8 uncovers the fundamental STTC encoder representation for M -PSK systems.

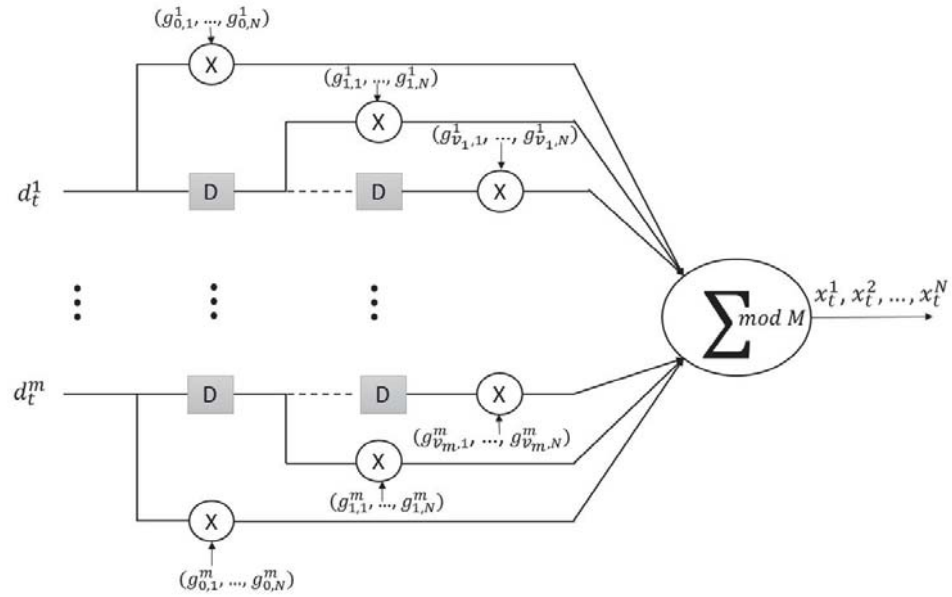


FIGURE 8. STTC Encoder for M -PSK Systems.

The rationale behind the shift register is as per the following. To begin with, the symbol d_t at time t is taken and subdivided into its bit pairs individually. They are reproduced by a constraint from the generator matrix in the wake of passing from every shift register individually. The number of the states is

defined according to the number of the registers. v number of registers give a 2^v number of trellis states. The Figure 9 represents the STTC performance regarding to number of states over flat fading channel.

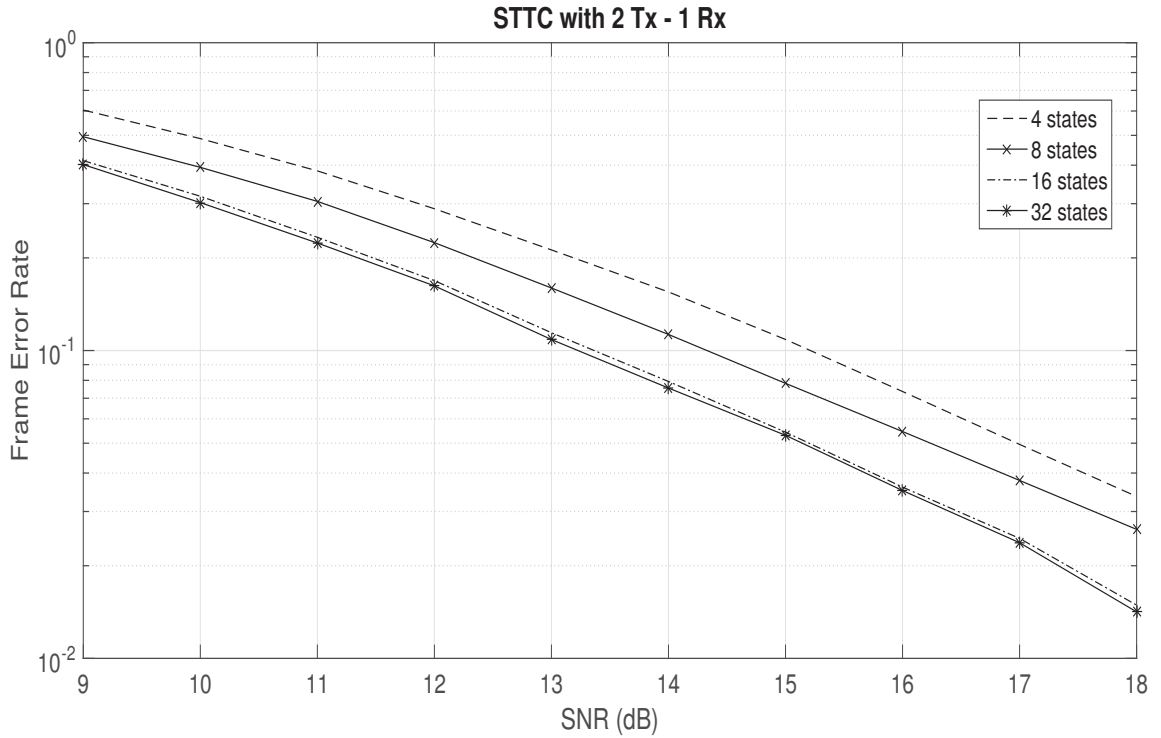


FIGURE 9. STTC for QPSK with 2 Transmit and 1 Receive Antenna.

There are a few generator matrix representations which are accomplished in various different ways. The most important rule for the generator matrix may be the setting the zeros for the beginning and the end of the data sequence to make sure that the generator matrix always starts and stops at the zero state. The points of interest for the code development can be found from Jankiraman [15]. In this thesis, the rank & determinant criteria is considered which is attained to by calculating the PEP.

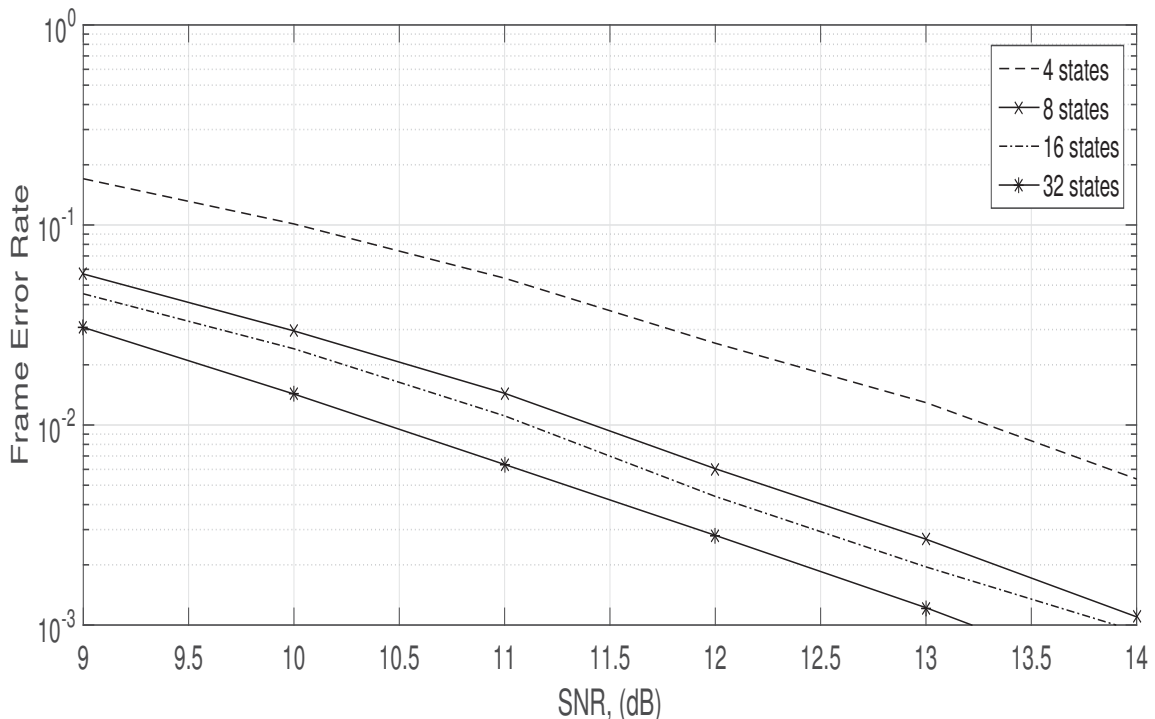


FIGURE 10. STTC for QPSK with 2 Transmit and 2 Receive Antenna.

4-state QPSK STTC Example

With a specific end goal to understand how the STTC works, it is critical to give a case for this. Assume a 4-state QPSK STTC encoder for $N = 2$ transmit antennas. The generator matrix for every transmit antenna can be offered according to rank & determinant criteria by, $g^1 = [(0, 2), (2, 0)]$ and $g^2 = [(0, 1), (1, 0)]$.

The 4-state trellis from Figure 5 can be connected here, and one can see four separate branches from every node, which is called as a state. The mapping of the symbols from the trellis can be discovered via careful observation of this in the Figure 5. Consider a serial bit stream ($d_t = 11, 01, 01, 10, 01, 00\dots$). The output sequence after going through the STTC encoder is ($x_t = 03, 31, 11, 12, 21, 10\dots$). The left symbol from every symbol pair in x_t is transmitted from 1st transmit

antenna. So also, the right one is from 2^{nd} transmit antenna. Subsequently, the transmitted sequences are $x_1^t = (0, 3, 1, 1, 2, 1, \dots)$ and $x_2^t = (3, 1, 1, 2, 1, 0, \dots)$. x_1^t and x_2^t are simply the mapped variant of QPSK symbols. As it were, the numbers $(0, 1, 2, 3)$ are transmitted as a QPSK complex symbol $(1, +j, -1, -j)$, respectively.

STTC Performance Analysis and Design Criteria

There are various sorts of designing criteria proposed for STTCs. Rank & determinant criteria [3] and trace criteria [16] are the most well known systems. In this section, just rank & determinant criteria strategy is clarified and utilized as a part of the simulation model. This section will show how to lead the space-time trellis codes utilizing this technique.

Most importantly, every case transmitted from every antenna is expected to have K symbols. Consider the $N \times K$ transmitted codeword matrix, provided in the wake of arranging the transmitted code sequence, as

$$X = [x_1, x_2, \dots, x_t, \dots] = \begin{pmatrix} x_1^1 & x_2^1 & \dots & x_K^1 \\ x_1^2 & x_2^2 & \dots & x_K^2 \\ \vdots & \vdots & \ddots & \vdots \\ x_1^N & x_2^N & \dots & x_K^N \end{pmatrix}_{N \times K} \quad (3.8)$$

where every row shows the transmitted codeword from every antenna. The space-time concept is characterized by every row of the transmitted codeword from equation 3.8. The pairwise error probability $P(X, \hat{X})$ is characterized as the likelihood of the incorrectly decoded code sequence $\hat{X} = [\hat{x}_1, \hat{x}_2, \dots, \hat{x}_t, \dots]$ from the first transmitted codeword $X = [x_1, x_2, \dots, x_t, \dots]$. Also, \hat{x} can be seen in equation

3.9.

$$\hat{X} = [\hat{x}_1, \hat{x}_2, \dots, \hat{x}_t, \dots] = \begin{pmatrix} \hat{x}_1^1 & \hat{x}_2^1 & \dots & \hat{x}_K^1 \\ \hat{x}_1^2 & \hat{x}_2^2 & \dots & \hat{x}_K^2 \\ \vdots & \vdots & \ddots & \vdots \\ \hat{x}_1^N & \hat{x}_2^N & \dots & \hat{x}_K^N \end{pmatrix}_{N \times K} \quad (3.9)$$

Consider the transmitted and the mistakenly received codewords to determine the inequality as,

$$\sum_{t=1}^K \sum_{j=1}^M |y_t^j - \sum_{i=1}^N h_{j,i}^t x_t^i|^2 \geq \sum_{t=1}^K \sum_{j=1}^M |y_t^j - \sum_{i=1}^N h_{j,i}^t \hat{x}_t^i|^2. \quad (3.10)$$

This inequality can be further written as,

$$\sum_{t=1}^K \sum_{j=1}^M 2\text{Re}\{(n_t^j)^* - \sum_{i=1}^N h_{j,i}^t (\hat{x}_t^i - x_t^i)\} \geq \sum_{t=1}^K \sum_{j=1}^M \left| \sum_{i=1}^N h_{j,i}^t (\hat{x}_t^i - x_t^i) \right|^2. \quad (3.11)$$

Here, the $\text{Re}\{\bullet\}$ is the real part of the complex number. If one assumes that the ideal CSI data is accessible at the receiver, the fading channel coefficients can be demonstrated as a matrix sequence of $H = [H_1, H_2, \dots, H_t, \dots]$. With this, the right hand side of the equation 3.11 turns into a steady, which is an altered version of the Euclidean distance between the code word matrices X and \hat{X} . This altered distance can be spoken to as $d^2(X, \hat{X})$. In this manner, the pairwise error probability can be gotten from

$$P(X, \hat{X}|H) = Q\left(\sqrt{\frac{E_s}{2N_o}} d^2(X, \hat{X})\right). \quad (3.12)$$

E_s and $Q(\bullet)$ represent every transmit antenna and the cumulative distribution function respectively. $Q(\bullet)$ can be recalled as

$$Q(x) = \frac{1}{\sqrt{2\pi}} \int_x^\infty e^{-\frac{t^2}{2}} dt. \quad (3.13)$$

The equation 3.13 above can be utilized as an inequality format by

$$Q(x) \leq \frac{1}{\sqrt{2}} e^{-\frac{x^2}{2}}, x \geq 0. \quad (3.14)$$

Hence, the PEP revealed in equation 3.12 can be rewritten as

$$P(X, \hat{X}|H) = \frac{1}{\sqrt{2}} \exp(-d^2(X, \hat{X}) \frac{E_s}{4N_o}). \quad (3.15)$$

Rank & Determinant Criterion

In the wake of giving the PEP depiction, the STC code design can be pictured simpler. The rank & determinant criterion was the first method to design STCs. Tarokh et al. [3] gives a comprehensive study about this. This standard is the way to characterize the diversity and the coding gain. Thus, the codeword difference matrix term is utilized to think that its rank and determinant to indicate the diversity and the coding gain.

The codeword difference matrix is the difference between the transmitted and the received codewords element by element. It can be characterized by

$$B(X, \hat{X}) = [X - \hat{X}] = \begin{pmatrix} x_1^1 - \hat{x}_1^1 & x_2^1 - \hat{x}_2^1 & \dots & x_K^1 - \hat{x}_K^1 \\ x_1^2 - \hat{x}_1^2 & x_2^2 - \hat{x}_2^2 & \dots & x_K^2 - \hat{x}_K^2 \\ \vdots & \vdots & \ddots & \vdots \\ x_1^N - \hat{x}_1^N & x_2^N - \hat{x}_2^N & \dots & x_K^N - \hat{x}_K^N \end{pmatrix}_{N \times K}. \quad (3.16)$$

From the equation 3.16, $N \times N$ codeword difference matrix $A(X, \hat{X})$ can be derived as

$$A(X, \hat{X}) = B(X, \hat{X}) \times B^H(X, \hat{X}) \quad (3.17)$$

where the term $(\bullet)^H$ represents the conjugate transpose (Hermitian) transformation.

If the number of independent subchannels $r \times M$ is small, the upper bound PEP condition from equation 3.11 can be simplified as

$$P(X, \hat{X}|H) \leq \left(\prod_{l=1}^r \lambda_l \right)^{-M} \left(\frac{E_s}{4N_o} \right)^{-rM} \quad (3.18)$$

for slow Rayleigh fading channel with the high SNR [3]. r is the rank of matrix $A(X, \hat{X})$, and $\lambda_l = \lambda_1, \lambda_1, \lambda_2, \dots, \lambda_r$ represents the non-zero eigenvalues of matrix $A(X, \hat{X})$.

Upper bound of the code frame error probability (FER) can be registered utilizing a union bound method [3]. This frame error probability incorporates the expansion of the all conceivable pairwise error probabilities over all error occasions. An exponential decrease can be seen in the PEP in equation 3.18 on account of an increment in SNR. Along these lines, the FER at high SNRs is ruled by the PEP with the base item $r \times M$, which is likewise called as diversity gain. Hence, it is alluring to maximize the minimum rank r to attain to great performing codes. Moreover, one can see from the PEP that the minimum product of the eigenvalues $\prod_{l=1}^r \lambda_l$ of the matrix $A(X, \hat{X})$ along the codewords sets ought to be maximized to reduce the error probability with the minimum rank. From an $N \times N$ matrix $A(X, \hat{X})$, the most extreme achievable rank r is N . Thus, the

maximum diversity of general system can be $N \times M$, which is normally not achievable because of the limitations on coding structures.

Hence, Tarokh et al. [3] shows a few perceptions for small values of rank $r \times M$ for slow Rayleigh fading channels in space-time code design. To start with, the rank r of matrix $A(X, \hat{X})$ should to be maximized over all sets of different codewords. Secondly, the minimum product of the eigenvalues $\prod_{l=1}^r \lambda_l$ ought to be maximized alongside the possible codeword sets with the minimum rank. This condition is called as rank & determinant criteria.

CHAPTER 4

OFDM SYSTEMS

Overview of the OFDM Systems

As shown in chapter 2, a mobile radio channel is depicted by a multipath fading (tap-channel model) environment. In a manner of speaking, the signal offered to the receiver contains a direct LOS radio wave, and additionally innumerable radio waves that arrive at the receiver at different times. Outside objects, for example, trees, hills, structures are the reasons behind reflection of the LOS signal, which have different arrival time at the receiver. These reflections bring about interference between the LOS signal and reflected signals. This interference is known as inter-symbol interference (ISI). To prevent ISI, the orthogonal subcarrier packet transmission principle is embraced on account of OFDM properties.

Orthogonal frequency division multiplexing (OFDM) is a broadly utilized system for encoding data as a part of numerous digital broadband communication system far and wide. It is utilized for both wired and wireless digital information transmission and has discovered application in WLAN (wireless local access network IEEE 802.11a,g,n,ac), ADSL and VDSL (asymmetric and very-high-bit-rate digital subscriber lines) with the name of discrete-multitone (DMT), and numerous more systems and products. OFDM is favored because of the preferences it is giving.

Above all else, it gives high spectral efficiency because of nearly separated orthogonal sub-carriers. By virtue of its orthogonality property and Fourier

transform properties, frequency selective multipath channel can be transformed into an individual flat fading channel relating to every subcarrier. It also provides much simpler equalization compared to other methods [10].

Nonetheless, OFDM has several disadvantages that must be tended to when its utilization is considered. Carrier frequency offset at the receiver, high peak to average power ratio (PAPR) and sensitivity to Doppler shift are the major flaws of OFDM.

Keeping in mind the end goal to overcome these issues, several effective arrangements are offered. One of them is utilizing OFDM with channel coding. Similarly, multiple antenna transmission is also proposed for OFDM with the name of MIMO-OFDM systems with different variations [6], [17]. This work will concentrate only on MIMO-OFDM arrangement part. Particularly, space-time trellis codes, consolidated with OFDM are demonstrated in this chapter.

Mathematical Model of a Traditional OFDM System

OFDM is based on parallel data transmission to combat multipath fading. The parallel data are made out of nearly spaced subcarriers which are sent simultaneously at the same time with the different carrier frequency.

The number K of the parallel streams is controlled by the prerequisites on the system and speaks to the number of sub-carriers utilized by the OFDM transmission. Higher values for K cause that a more extensive bandwidth will be utilized and a higher data rate can be achieved. However, this takes a swing at a higher computational cost and increased necessities for the digital signal processors on both the transmitter and receiver. The K parallel symbol streams will then be handled by a K -point inverse Fourier transformation block that will generate K parallel channel yields which then need to be further changed over to a serial stream and transmitted. The main characteristic of OFDM is that the subcarriers

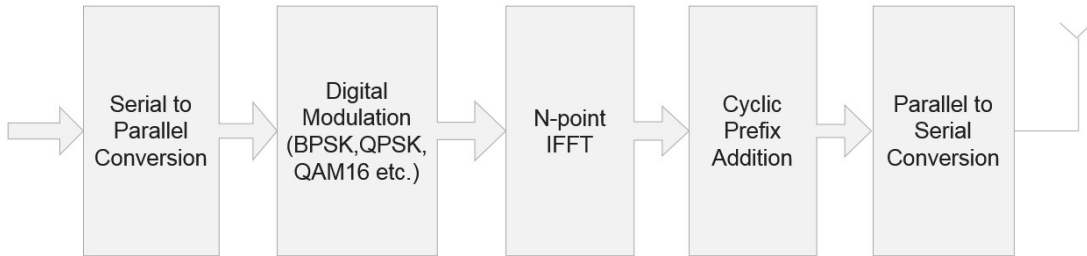


FIGURE 11. Traditional OFDM Transmitter Block Diagram.

are orthogonal to each other which allows them to be spaced closer to each other. This closer spacing allows for smaller overall bandwidth compared to other frequency division multiplexing systems. The orthogonality of the sub-carriers is maintained by the equation of the IFFT used to modulate the K parallel data.

As can be seen from Figure 11, the serial data sequence is changed over into K parallel branches right away. After applying digital modulation with a sort of phase shift keying (PSK) or quadrature amplitude modulation (QAM), each branch is applied to K -point inverse fast Fourier transform (IFFT) so as to enter to the time domain channel with different frequencies via orthogonal sub-carriers which is represent by,

$$x_k = \sum_{n=0}^{K-1} d_n e^{j2\pi nk/K} \quad k = 0, 1, \dots, K - 1. \quad (4.1)$$

In equation 4.1, d_n represents the each modulated symbols, and $e^{j2\pi nk/K}$ corresponds the orthogonal frequencies of the each sub-carrier. Next, to prevent ISI between each sub-carrier, a compensation area is added to the start of each sub-carrier. This method is called as cyclic prefix. To guarantee that the symbols are not going to interfere with each other, the end part of the each symbol which

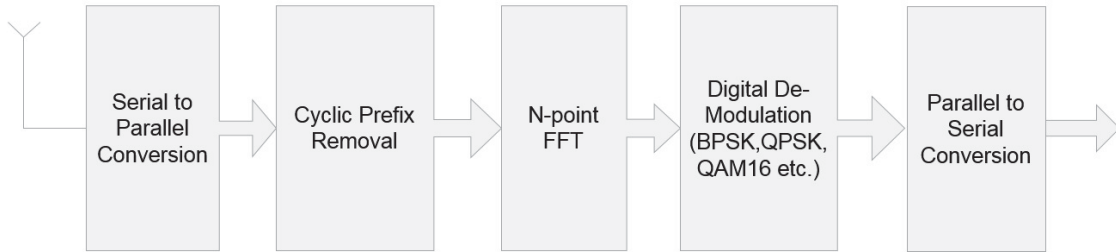


FIGURE 12. Traditional OFDM Receiver Block Diagram.

must have a greater time duration than the delay spread of the channel are added to the starting. Afterwards, the cyclic prefix added K sub-carriers are converted into a serial data stream with parallel to serial converter to be transmitted into the channel. Subsequently, the regular time domain convolution is changed over into circular convolution.

Once the signal is transmitted through the channel, it is received at the receiver with the addition of the AWGN noise, and it is changed over to K -parallel stream to make reverse operations for each sub-carrier as in Figure 12. Firstly, the added cyclic prefix is expelled from the beginning of the data packet. Next, each sub-carrier is applied by K -point fast Fourier transform (FFT) as seen in equation 4.2.

$$\hat{d}_n = \frac{1}{K} \sum_{k=0}^{K-1} x_k e^{-j2\pi nk/K} \quad n = 0, 1, \dots, K - 1. \quad (4.2)$$

Before the demodulation stage, there is a need for making a channel compensation, which is also called as channel equalization. Assuming the channel state information (CSI) is known, the channel compensation is simply started with the use of K -point FFT of the impulse response of the each channel. The channel compensation is therefore provided by the division of each received sub-carrier

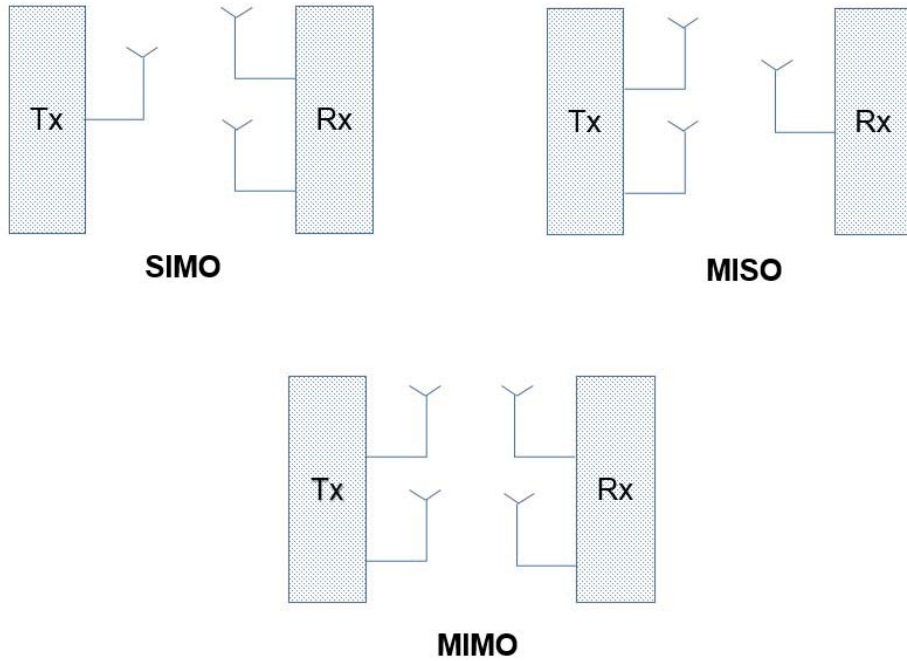


FIGURE 13. Multiple Antenna Transceiver Block Diagram.

with equivalent channel sub-carrier $d_n = \hat{d}_n / H_n$ which are taken from equations equation 4.2 and equation 4.3. h_k in equation 4.3 is taken from the tap channel model equation 2.8. In the simulation models, the channel compensation cannot be applied due to unknown reasons. As soon as it is fixed, the channel compensation will provide numerous application to add to overall system.

$$H_n = \sum_{k=0}^{K-1} h_k e^{-j2\pi nk/K} \quad n = 0, 1, \dots, K - 1. \quad (4.3)$$

After the channel compensation on the each sub-carrier, the K -point parallel stream is again changed over into serial stream. It takes after demodulation, and the signal is gotten with a few errors. Here, the OFDM system is presented briefly. The details about OFDM can be found from Cho et al. [7].

MIMO-OFDM Channel Models

After providing the main concepts relating to the OFDM, it is convenient to derive the same OFDM concept into multiple antenna communication. Figure 13 indicates the block diagram of SIMO, MISO and MIMO systems.

At the point when the OFDM framework is added to these various antenna configurations, one can essentially apply the same rule with what the traditional OFDM requires. In summary, IFFT block is added to the transmitter. Cyclic prefix is then attached to each frame. Next, the signal is transmitted over an optional number of transmit antenna and received by the optional number of receive antennas. Next, the AWGN noise is added. The cyclic prefix is removed. At that point, the FFT block is added to the receiver. The channel is compensated. Finally, the signal is demodulated, and the operation is finished. With the utilization of space-time codes, the things become more complicated. Next chapter is going to consolidate space-time codes, in particular space-time trellis codes and OFDM.

CHAPTER 5

THE SIMULATION OF STTC-OFDM OVER FREQUENCY SELECTIVE FADING CHANNEL MODEL

STTC-OFDM Simulation Parameters

Consider an OFDM framework with $N = 2$ transmit antennas, $M = 1$ receive antenna and $K = 256$ sub-carriers with 1 mega Hertz (MHz) of bandwidth. These relate to a subchannel separation of 3.9 kHz. One OFDM frame takes 256 microseconds (μs). With a specific end goal to combat the multipath channel effect, 40 μs of cyclic prefix is appended to each frame. The channel is assumed as 2-tap frequency selective model. The Doppler effect on the performance is also viewed as in contrast to without Doppler effect. At the point when the Doppler frequency is thought of it as, is assumed as 200 Hz. Space-time trellis codes are assumed to utilize QPSK modulation with 16-states STTC encoder. The generator matrix and rank & determinant criteria are assumed for the space-time code generation [3]. The Figure 14 represents the main simulation model which is studied to offer the results comparison according to different criteria.

This chapter explains the STTC-OFDM model in three section. In order to complete the model, everything is needed to be followed carefully. So, the blueprint of this system is given by the following three sections.

STTC-OFDM Transmitter

Assume a random binary sequence b_k which is initially modulated with the QPSK modulator. The symbol sequence d_k for time k is produced. Next, d_k is sent to the STTC encoder which utilizes 16-states generator matrix [15]. The symbol

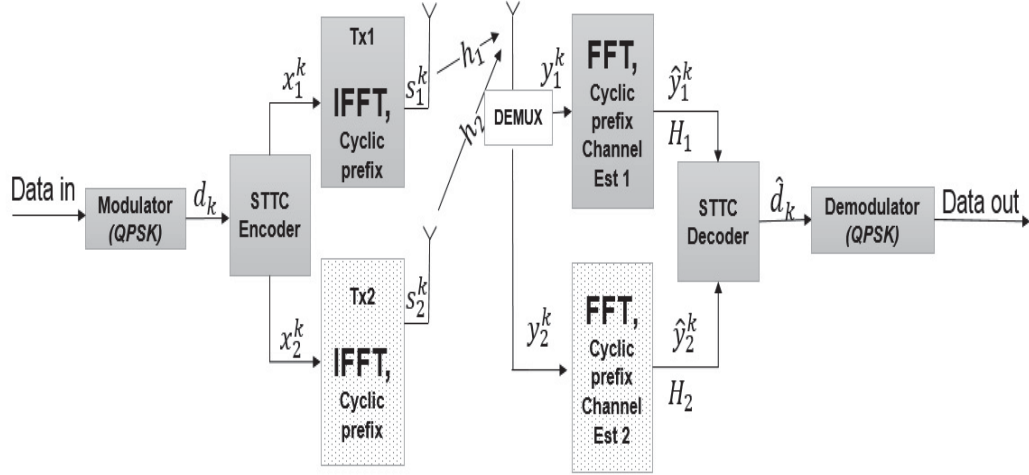


FIGURE 14. 2-Tx & 1-Rx STTC-OFDM System.

sequence d_k is changed over into two branches x_1^k and x_2^k to be transmitted from antenna 1 and antenna 2, separately. At that point, IFFT with 256 subcarriers is connected to x_1^k and x_2^k at every transmit antenna. Cyclic prefix is followed by IFFT. As indicated by the system sampling time, every subcarrier takes $1 \mu s$. Thus, last 40 subcarriers of every transmitted bundle is included toward the start of the same parcel. This cyclic prefix can be reviewed from the previous chapter to comprehend why it is utilized. At that point, the cyclic prefix included IFFT symbols s_1^k and s_2^k are sent in the same package in the meantime.

STTC-OFDM Channel Model

As the second chapter clarifies the fading and the AWGN channels, they are additionally utilized as a part of the system acknowledgement. Consider the system with the 2-taps. The results were provided for 2-tap channels with the delay spread of $5 \mu s$. Besides, the AWGN channel is utilized with the 3 dB attenuation. The AWGN ought to be demonstrated by paying attention on multiple antenna power principle.

2-tap Frequency Selective Fading Channel

The 2-tap channel model can be utilized from the mathematical statement equation 2.8. The transmitted sequences s_1^k and s_2^k are convolved with the fading channels, which are the channel representation between every transmit antenna and receive antenna respectively. The channel coefficient h_1 speaks to the channel between the first transmit antenna and the receive antenna. Likewise, h_2 is the channel between the second transmit antenna and the receive antenna. s_1^k is convolved with h_1 . Also, s_2^k is convolved with h_2 . Every transmitted sequence has 296 subcarriers because of the cyclic prefix which takes 296 μs .

AWGN Channel

As it is talked about in the Chapter 2, the AWGN channel is calculated by attenuation variable. This is the part where the signal to noise ratio concerns for its calculation. The attenuation is calculated for the MISO system as follows:

$$spow = 0.5 \times \left((y_1^k \times (y_1^k)^*) + (y_2^k \times (y_2^k)^*) \right) / 296 \quad (5.1)$$

After the signal power $spow$ is calculated. The $3dB$ attenuation can be calculated by,

$$attn_{3dB} = \sqrt{0.25 \times spow \times 10^{-\frac{(E_b/N_o-3)}{10}}} \quad (5.2)$$

At that point, a Gaussian random noise is produced for every received subcarrier. This is multiplied with the $attn_{3dB}$ from equation 5.2. It is added to each received subcarrier. This noise is independent for every subcarrier. Equations equation 5.1 and equation 5.2 are applied to each received subcarrier.

STTC-OFDM Receiver

In the wake of passing the frequency selective channel and being joined with the AWGN channel, the corrupted signal is begun to be processed at the receiver part. Initially, with a specific end goal to process the received signal from the every transmit antenna individually, the received signal is entered to a basic demultiplexer (DEMUX) circuit so every received signal will be handled further as y_1^k and y_2^k . Next, the first 40 subcarriers are expelled from y_1^k and y_2^k since they are the cyclic prefix part. After removing the cyclic prefix, every received signal y_1^k and y_2^k are connected to the FFT block to reverse the operations in the transmitter. At that point, as indicated by OFDM scheme, there ought to be a requirement for a channel compensation with the utilization of K -point FFT of the channel coefficients. On the other hand, the simulations demonstrate that the STTC decoder part is giving the channel compensation too. It implies that there is no compelling reason to any extra compensation or equalization to the received signal after being applied FFT. y_1^k and y_2^k are essentially added one to another.

The STTC decoder is connected by the subcarriers separately. Review that the conventional flat fading STTC was decoding the y_t sequence with the utilization of just single coefficient to find the each possible trellis path for branch metric calculations. Moreover, if the OFDM is added to the system, the frequency selective channel is changed over to multiple flat fading channels. When they are combined, one can utilize the K -point FFT of the every channel coefficients. Consequently, the channel coefficients h_1 and h_2 are utilized as H_1 and H_2 after FFT is applied. At that point, every subcarrier is decoded by the equivalent channel subcarrier coefficient from H_1 for y_1 and from H_2 for y_2 . The STTC

decoder equation 3.7 can be adjusted as takes after:

$$\hat{d}_k = \sum_{k=0}^{K-1} \sum_{j=1}^M |\hat{y}_j^k - \sum_{i=1}^N H_{j,i}^k q_k^i|^2. \quad (5.3)$$

With a specific end goal to make the equation 5.3 more clear, the extra clarifications may be given. The H has 256 components. It speaks to the frequency response of the channel h . The decoding algorithm meets expectations only if it is applied for each subcarrier individually. In other words, every received subcarrier \hat{d}_k picks the shortest branch metric which is calculated with the k^{th} subcarrier coefficient of the H_k . At that point, the Viterbi algorithm can be applied after picking the shortest branch metric for the each subcarrier as same as the regular STTC in equation 3.7.

STTC-OFDM Versus ST-OFDM

In this section, the STTC-OFDM system is analyzed and contrasted with regard to two criteria. The main criterion is considered with a specific end goal to perceive the frame error rate (FER) change. The STTC-OFDM is compared with the regular space-time OFDM (ST-OFDM) in [17]. The ST-OFDM system is outlined according to [17], yet all the system parameters, such as, the number of subcarriers, sampling time, cyclic prefix are situated by for focusing all the more on previous STTC based performance. Also, STTC-OFDM system performance is accommodated for different Doppler frequencies under the conditions above. The Doppler frequency is analyzed by two scenarios. First case represents without Doppler frequency. In other words, the Doppler frequency is $f_D = 0Hz$. The second one shows with Doppler frequency case which is $f_D = 200Hz$.

STTC-OFDM Versus ST-OFDM without Doppler Frequency

As the Doppler frequency is set to $f_D = 0Hz$, the simulation result demonstrates the trellis coding effect on the space-time system model very clear. The Figure 15 is the reproduction result for $f_D = 0Hz$ which highlights that the more E_b/N_o , the more the FER improvement.

A few observations can be accommodated for this result. First of all, the STTC-OFDM system is just given until the $FER = 10^{-2}$ level of the previous studies [6]. By making the examination between ST-OFDM and STTC-OFDM uncovers that the coding gain can altogether enhance the space-time coding as the FER level declines underneath the $FER = 10^{-2}$ level. At the FER level of 10^{-4} , STTC-OFDM provides 4 dB better than the ST-OFDM system, which is quite an outstanding result. That is the motivation behind why the STTC-OFDM is more preferable than the ST-OFDM in the high E_b/N_o levels in the case of no Doppler frequency.

STTC-OFDM Versus ST-OFDM with Doppler Frequency

At the point when the Doppler frequency is $f_D = 200Hz$, the FER performance is significantly degraded. This is an expected phenomenon. This thesis covers the STTC-OFDM system with respect to the first study about this [6]. Tarokh in [6] tells that a Doppler frequency $f_D = 200Hz$ is utilized as a part of the system.

However, the simulation results in this thesis prove that the provided result to 2-tap channel with $5\mu s$ delay spread in [6] did not pursue any Doppler frequency. The provided result to 2-tap channel with $5\mu s$ in [6] precisely matches with the previous case of without Doppler frequency. The Figure 16 shows the STTC-OFDM and ST-OFDM performance under the Doppler frequency $f_D = 200Hz$.

Also, there is an interesting consequence to be observed as long as the delay spread between the two paths of the channel is increased. When the delay spread is taken as $40\mu s$, the STTC-OFDM performance is improved much more compared to they regular ST-OFDM system. The Figure 17 reveals their performance comparison with $40\mu s$ delay spread.

It can be observed that the Doppler frequency adversely influences the system. The STTC-OFDM is as yet giving preferable execution over ST-OFDM. One can see the coding gain effect on space-time systems with respect to STTC-OFDM. Besides, the increase in the delay spread results in more STTC-OFDM performance. It is because of the fact that the coding gain gets better with the bigger delay spread.

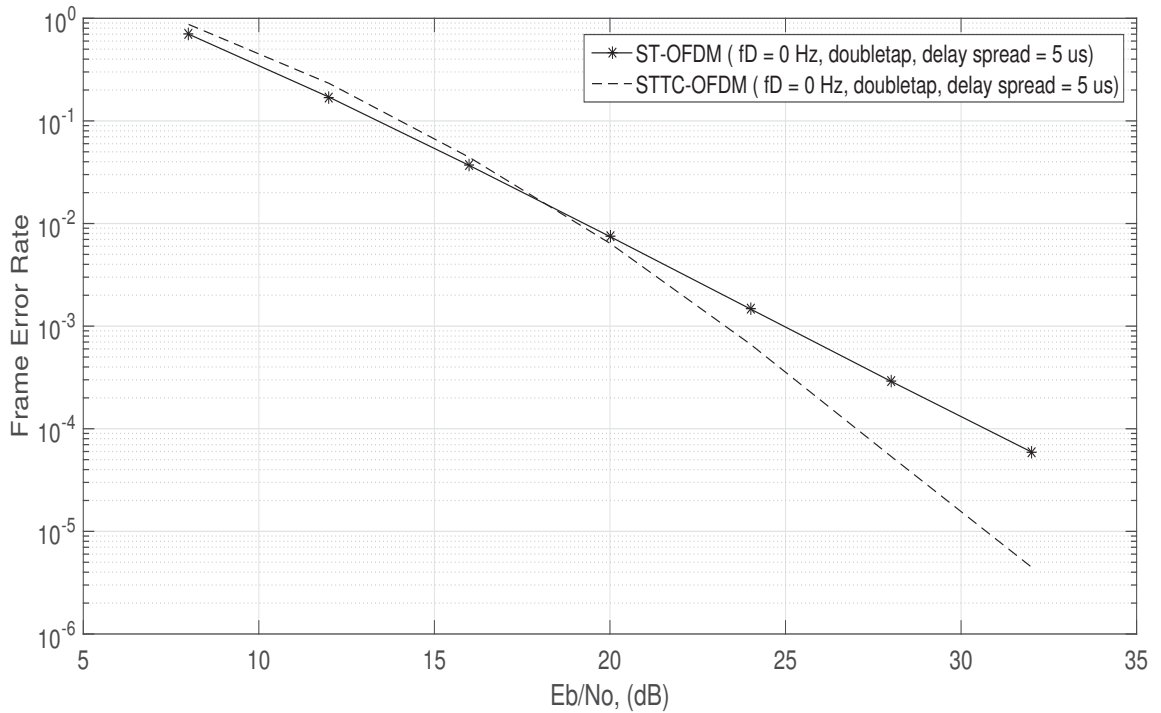


FIGURE 15. ST-OFDM vs STTC-OFDM with $f_D = 0Hz$.

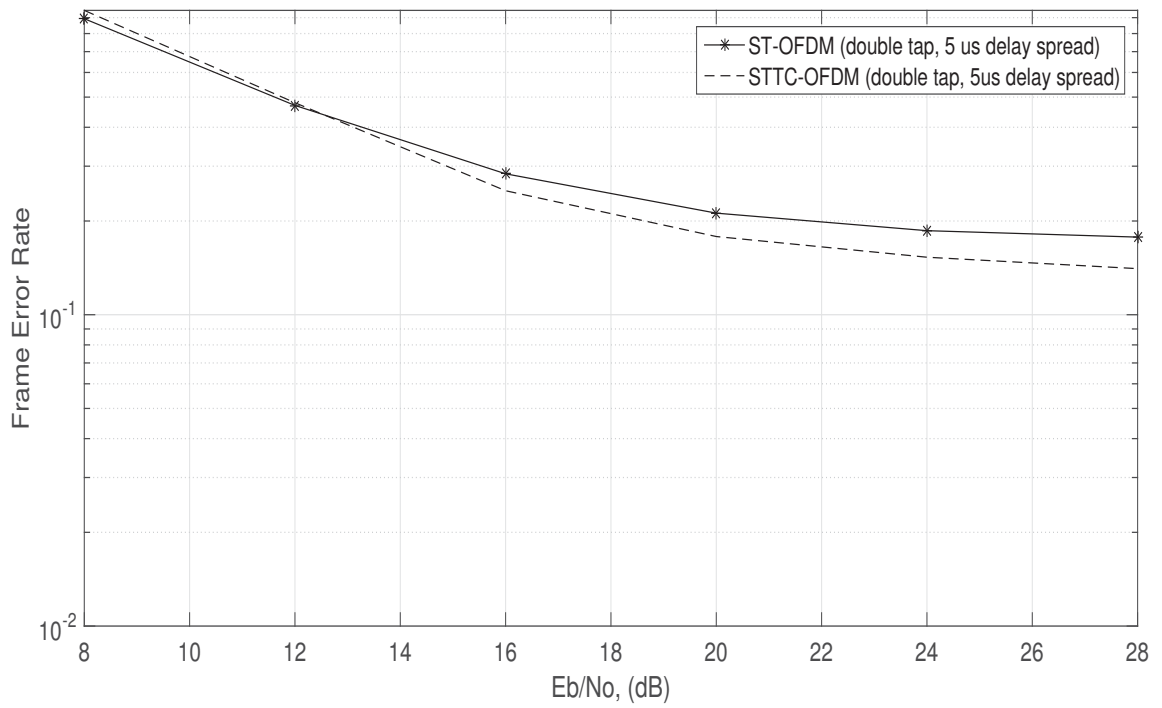


FIGURE 16. ST-OFDM vs STTC-OFDM with $f_D = 200Hz$ ($5\mu s$ delay spread).

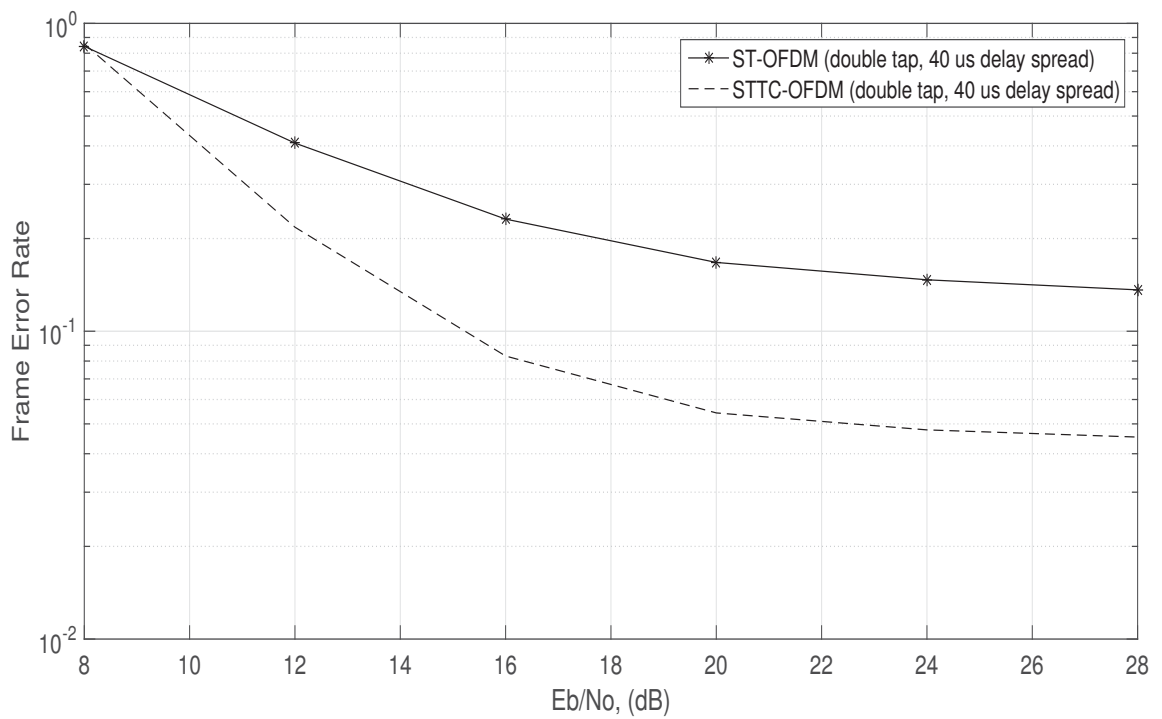


FIGURE 17. ST-OFDM vs STTC-OFDM with $f_D = 200Hz$ ($40\mu s$ delay spread).

CHAPTER 6

THE FUTURE IMPLEMENTATIONS FOR STTC-OFDM SYSTEMS

In this section, STTC-OFDM system can be further extended with the smart alterations. The idea is taken from [8]. So as to know the acceptable distinction between the proposed systems and the current system, it is good to begin with the fundamental ST-OFDM system and STTC-OFDM system which are compared in the previous chapter.

The Figure 18 shows the regular ST-OFDM system block diagram as the first reference model of the space-time coded OFDM transmission. The distinction of ST-OFDM with the STTC-OFDM can be figured out in [17], [6]. One can review that the Figure 14 demonstrates the STTC-OFDM block diagram.

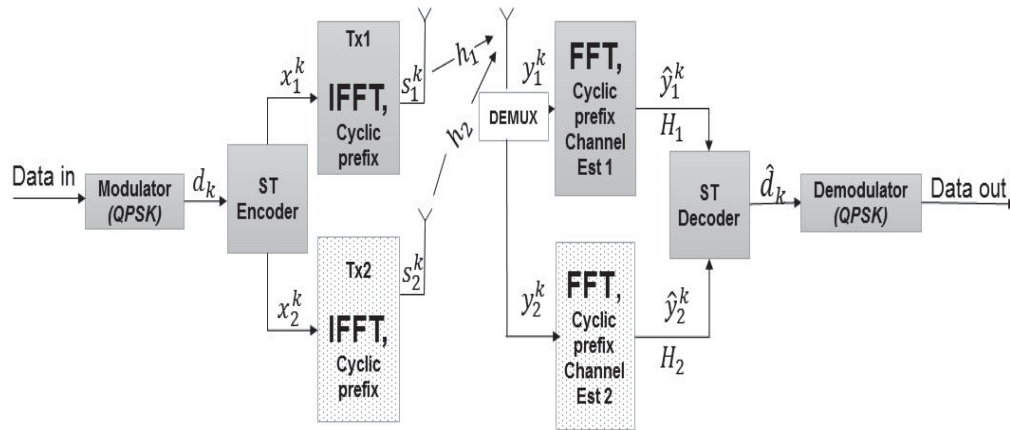


FIGURE 18. 2-Tx & 1-Rx Regular ST-OFDM System.

After carefully observing these two figures and Yeh's paper [8], conjugate and parallel cancellation can be connected to the STTC-OFDM systems. Three

new systems are executed with the ideas of the parallel cancellation, the conjugate cancellation and the conjugate parallel cancellation.

STTC-PC-OFDM Systems

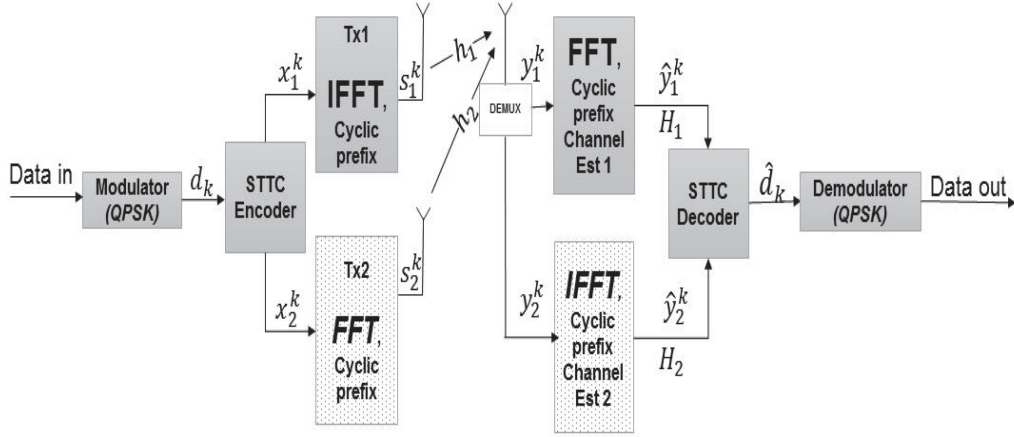


FIGURE 19. 2-Tx & 1-Rx STTC-PC-OFDM System.

The initially proposed system is space-time trellis coded parallel cancellation OFDM (STTC-PC-OFDM). The idea behind the STTC-PC-OFDM system is clarified as takes after:

Regular ST-OFDM ($2Tx \times 1Rx$) has an IFFT block at the every transmit branch. Likewise, the receiver applies an FFT operation for every received sequence as can be seen from the Figure 18. Parallel cancellation is basically given by changing one of the two IFFT blocks to FFT at the receiver side, and vice versa at the receiver. The Figure 19 envisions the STTC-PC-OFDM ($2Tx \times 1Rx$) system. The STTC-OFDM concept about channel compensation is still utilized here. The main thing is to apply IFFT to channel frequency response of the receiver rather than FFT to finish parallel cancellation schemes. H_2 which is the

utilized channel for the parallel transmitted branch in the figure speaks to the $IFFT(h_2)$ to complete the picture.

STTC-CC-OFDM Systems

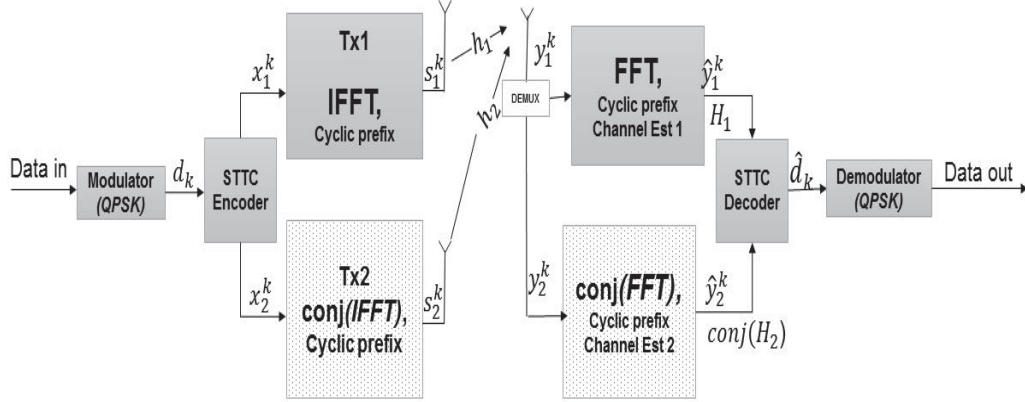


FIGURE 20. 2-Tx & 1-Rx STTC-CC-OFDM System.

The parallel cancellation can be changed with the conjugate cancellation. It just applies the conjugate operation to the second branch of the transmitter and again apply the conjugate operation on the receiver side including the channel frequency response. The Figure 20 exhibits the proposed STTC-CC plan. To finish the trellis decoding, H_2 is taken as $conj(FFT(h_2))$.

STTC-CPC-OFDM Systems

One can think that both parallel cancellation and conjugate cancellation can be joined together to the STTC-OFDM system to enhance the proposed system further. The Figure 21 demonstrates the last form of the proposed system.

Fundamentally, the extension which the parallel cancellation is connected is likewise consolidated with the conjugation. On the off chance that one applies the parallel and the conjugate operation to the same extension, the outcome gives the

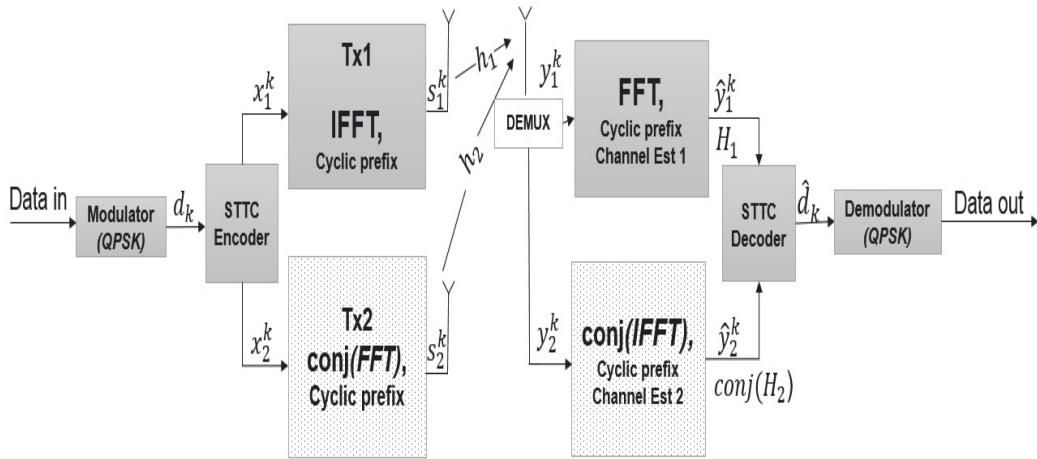


FIGURE 21. 2-Tx & 1-Rx STTC-CPC-OFDM System.

proposed STTC-CPC-OFDM system. Eventually, it gives somewhat preferred performance over STTC-PC and STTC-CC.

Future Works

Even though, the three new proposed systems are not superior to regular STTC-OFDM, they can be analyzed further to make them superior to it. As the simulations are provided, STTC-OFDM does not allow to apply channel compensation, which is actually needed for any MIMO-OFDM applications. There are some doubts about a few things. The channel compensation effect can be provided in the STTC decoder part, since the STTC decoder uses the channel frequency response at the each subcarrier to calculate the possible trellis path. We suspect that if the channel compensation is somehow provided which gives the desired STTC-OFDM performances, all these new proposed systems will show their effect to bolster the system further. Besides, if the channel compensation is again provided properly, we can also add some precoder applications to our space-time model.

According to our predictions, once the channel compensation is provided after applying the FFT at the each received branch, the STTC decoder can use the constant 1 as the channel coefficient because the compensation eliminated the channel effect. Once we apply this idea to the STTC decoder, the precoder applications such as the Walsh-Hadamard transform and Frank-Zadoff transform can show their effect. Nonetheless, the channel compensation makes the original system performance much worse. Though the precoder works properly, the system gives bad performance results. This is a reasonable topic to solve the channel compensation if it can be applied.

CHAPTER 7

CONCLUSION AND RECOMMENDATIONS

In this work, several models are studied with the use of STTC. The STTC-OFDM is a preferable option to improve the space-time code performance. During the system simulations, there are some issues that cannot be neglected. The first problem is to identify the decoder section for STTC-OFDM. The second problem is that the first STTC-OFDM [6] study considers the simulation parameters with the use of Doppler frequency. To figure out whether the Doppler frequency is really used or not, several comparisons between STTC-OFDM and ST-OFDM are provided to make a decision. After the first STTC-OFDM study [6], none of the papers does not mention about the Doppler frequency.

Secondly, when the OFDM is added to the system, there should be a channel compensation for the system in the receiver part. As the channel compensation is applied, the performance of the system is degraded significantly. However, it is observed that the channel compensation is automatically provided by the STTC decoder section of the receiver part. This thesis actually aimed at including Walsh-Hadamard transform to improve the overall system performance. Nonetheless, the Walsh-Hadamard transform and Frank-Zadoff transform can be applied after making the channel compensation. It interferes with the original STTC-OFDM design.

Last but not least, if the channel compensation is provided as discussed in the Chapter 6, the proposed systems STTC-PC-OFDM, STTC-CC-OFDM and STTC-CPC-OFDM can successfully improve the regular STTC-OFDM systems.

Furthermore, the block interleaver addition after the symbol generation at the transmitter part can contribute to the FER performance improvement in the STTC-OFDM systems.

REFERENCES

BIBLIOGRAPHY

- [1] G. J. Foschini, "Layered space-time architecture for wireless communication in a fading environment when using multiple antennas," *Bell Labs Technical Journal*, vol. 1, pp. 41-59, Autumn 1996.
- [2] J.H. Winters, "The diversity gain of transmit diversity in wireless systems with Rayleigh fading," in proceedings IEEE ICC94, USA, 1994, vol. 2, pp. 1121-1125.
- [3] V. Tarokh, N. Seshadri, and A. R. Calderbank, "Space-time codes for high data rate wireless communication: Performance criterion and code construction," *IEEE Transactions on Information Theory*, vol. 44, pp. 744-765, March 1998.
- [4] S. M. Alamouti, "A simple transmitter diversity scheme for wireless communications," *IEEE Journal on Selected Areas in Communications*, vol. 16, pp. 1451-1458, October 1998.
- [5] "Orthogonal Frequency Division Multiplexing," *U.S. Patent No. 3, 488, 4555*, filed November 14, 1966, issued Jan. 6, 1970.
- [6] D. Agrawal, V. Tarokh, A. Naguib and N. Seshadri, "Space-time coded OFDM for high data-rate wireless communication over wideband channels," in *Vehicular Technology Conference, 1998. VTC 98. 48th IEEE*, vol.3, no., pp.2232,2236, 18-21 May 1998.
- [7] Y. Cho, J. Kim, W. Yang and C. Kang, *MIMO-OFDM Wireless Communications with MATLAB*. Singapore: John Wiley & Sons (Asia) Pte Ltd, 2010.
- [8] H.G. Yeh and K. Yao, "A parallel ICI cancellation technique for OFDM systems," in *IEEE Global Communications Conference (GLOBECOM)*, 2012, pp.3679-3684.
- [9] B. Sklar, *Digital communications: Fundamentals and Applications*. Upper Saddle River, NJ: Prentice Hall Communications Engineering and Emerging Technologies Series, 2001.
- [10] H. Harada and R. Prasad, *Simulation and Software Radio for Mobile Communications*. Norwood, MA: Artech House, 2001.
- [11] T. Duman and A. Ghayeb, *Coding for MIMO Communication Systems*. Chichester, UK: John Wiley and Sons, 2007.

- [12] Yi Hong, Jinhong Yuan, Jinho Choi and Xun Shao, "Performance analysis of space-time trellis coded OFDM over quasi-static frequency selective fading channels," *Information, Communications and Signal Processing, 2003 and Fourth Pacific Rim Conference on Multimedia. Proceedings of the 2003 Joint Conference of the Fourth International Conference on* , vol.3, no., pp.1478,1482, 15-18 Dec. 2003.
- [13] A. Wittneben, "A new bandwidth efficient transmit antenna modulation diversity scheme for linear digital modulation," *Communications, 1993. ICC '93 Geneva. Technical Program, Conference Record, IEEE International Conference* , vol.3, no., pp.1630,1634 vol.3, 23-26 May 1993.
- [14] G.D., Forney, "The Viterbi algorithm," *Proceedings of the IEEE*, vol.61, no.3, pp.268,278, March 1973.
- [15] M. Jankiraman, *Space-Time Codes and MIMO Systems*. Norwood, MA: Artech House, 2004.
- [16] Z. Chen, J. Yuan, and B. Vucetic, "Improved space-time trellis coded modulation scheme on slow Rayleigh fading channels," *Electronics Letters*, vol. 37, no. 7, pp. 440-441, March 2001.
- [17] K.F. Lee and D.E. Williams, "A space-time coded transmitter diversity technique for frequency selective fading channels," *Proceedings of the IEEE Sensor Array and Multichannel Signal Processing Workshop*, pp. 149-152, March, 2000.